

Krylov Subspace Approximation for Local Community Detection

Kun He, *Member, IEEE*, Pan Shi, David Bindel, *Member, IEEE*, and John E. Hopcroft, *Life Fellow, IEEE*

Abstract—Community detection is an important information mining task in many fields including computer science, social sciences, biology and physics. For increasingly common large network data sets, global community detection is prohibitively expensive, and attention has shifted to methods that mine local communities, *i.e.* methods that identify all latent members of a particular community from a few labeled seed members. To address this semi-supervised mining task, we propose a local spectral subspace-based community detection method, called LOSP. A sampling technique is first applied around the seeds to significantly reduce the scale of the search. Then we define a family of local spectral subspaces based on Krylov subspaces, and seek a sparse indicator for the target community via an ℓ_1 norm minimization over the Krylov subspace. Variants of LOSP depend on types of random walks with different diffusion speeds, regular random walk or inverse random walk, dimension of the local spectral subspace and steps of diffusions. The effectiveness of the proposed LOSP approach is theoretically analyzed based on Rayleigh quotients, and is experimentally verified on a wide variety of real-world networks across social, production and biological domains, as well as on an extensive set of synthetic LFR benchmark datasets.

Index Terms—Local community detection, spectral clustering, Krylov subspace, Rayleigh quotient, sparse linear coding



1 INTRODUCTION

COMMUNITY detection has arisen as one of the significant topics in network analysis and graph mining. Many problems in information science, social science, biology and physics can be formulated as problems of community detection. However, exploring a network's *global* community structure [1], [2] becomes prohibitively expensive in networks with millions or billions of nodes. Hence, attention has shifted to methods that mine local community structure without processing all of a large network [3], [4], [5], [6].

In many situations, instead of finding all communities in a large network in an unsupervised manner, we just want to quickly find communities from a small set of members labeled by a domain expert. For example, in political participation networks, one might discover the membership of a political group from a few representative politicians [7]; sales websites might use clusters in co-purchase networks to generate product recommendations for a customer based on previous purchases; and starting from a few well-studied genes, biologists may seek functionally similar genes via genetic interaction networks.

Communities in real-world networks are often small, comprising dozens or hundreds of members [8], [9]. Intuitively, the latent members in these small communities should be very close to any example members. The *seed set expansion* approach to community detection [1], [10], [11] starts from "seed" nodes, or labeled members of a target

community [3], [4], [12], and incrementally grows the set by locally optimizing a community scoring function.

A common theme in seed set expansion methods is to diffuse probability from the seeds. PageRank [4], [13], heat kernel [12], [14] and local spectral approximation [15], [16] are three main techniques for the probability diffusion. Among these, the local spectral method is a newly proposed technique that exhibits high performance for the local community detection task. Motivated by standard spectral clustering methods that find disjoint communities from the leading eigenvectors of the graph Laplacian, local spectral algorithms seek a sparse indicator vector that contains the seeds and lies in a local spectral subspace.

We propose a local spectral (LOSP) algorithm to identify the members of small communities [15], and systematically extend the LOSP family based on various Krylov subspace approximations. LOSP differs from standard spectral clustering in two ways:

- **Handling overlapping communities.** Standard spectral methods partition a graph into disjoint communities by k -means clustering in a coordinate system defined by eigenvectors or by recursive spectral bisection. We instead use ℓ_1 -norm optimization to search an (approximate) invariant subspace for an indicator vector for a sparse set containing the seeds. Overlapping communities correspond to different seed sets.
- **Defining a local spectral subspace.** To determine the local structure around the seeds of interest, we calculate a local approximate invariant subspace via a Krylov subspace associated with short random walks. The vectors in the subspace are nearly zero except close to the seeds.

In this paper, we systematically develop a family of LOSP methods and provide theoretical analysis. Starting

-
- K. He and P. Shi are with the Department of Computer Science, Huazhong University of Science and Technology, Wuhan, China, 430074. P. Shi is the corresponding author.
E-mail: {brooklet60, panshi}@hust.edu.cn
 - D. Bindel and J. E. Hopcroft are with the Department of Computer Science, Cornell University, Ithaca, NY, 14853.
E-mail: {bindel, jeh}@cs.cornell.edu

Manuscript received November 24, 2017.

from a few random seeds, we sample locally in the graph to get a comparatively small subgraph containing most of the latent members, so that the follow-up membership identification can focus on a local subgraph instead of the whole network. The LOSP methods are then used to extract the local community from the sampled subgraph via a Krylov subspace formed by short-random-walk diffusion vectors.

Our main contributions include:

- **Sampling to reduce the complexity.** We sample locally in the graph as a pre-processing to get a much smaller subgraph containing most of the latent members around the seeds. The follow-up calculation has a low complexity while maintaining an accurate covering on the target community. In this way, the proposed method is applicable to the large-scale networks.
- **Building a rich LOSP family.** We systematically develop a family of local spectral methods based on random walk diffusion. We thoroughly investigate a rich set of diffusions; and we find that light lazy random walk, lazy random walk and personalized PageRank are robust for different parameters, and outperform the standard random walk diffusions. We also study the regular random walk diffusions spreading out from the seeds and the inverse random walk diffusions ending at the seeds.
- **Extensive demonstration of LOSP.** We provide a diverse set of computational experiments on 28 synthetic benchmark graphs and eight real-world social and biological networks to show that proposed methods are much more accurate than the well-known personalized PageRank diffusion algorithm `pprpush` [13] and heat kernel algorithm `hk-relax` [12].

2 RELATED WORK

Communities are densely intra-linked components with sparser inter-connections, typically defined by means of metrics like modularity [17] or conductance [18]. There are many different research directions as well as approaches for the community detection [19], [20], [21]. Early works focused on global structure mining [1], [2], [22] while an increasing body of recent work focuses on local structure mining [4], [6], [23]. We will focus on seed set expansion methods that uncover a local community from a few seed members; these were initially designed for global community detection, but have since been extensively used in local community mining. Our focus is the LOSP approach to seed expansion for community mining in static, undirected, unweighted networks. The task of finding communities by adapting LOSP in networks with dynamic structure [24] and signed and weighted edges [25] is future work, as is the extension of our methods to spectral subspaces based on clustering in geodesic space [26] and the use of new metrics to evaluate community quality [27].

Global seed set expansion. Many global community detection algorithms are based on seed set expansion. Clique Percolation [1], the most classical method, starts from maximal k -cliques and merges cliques sharing $k - 1$ nodes to form a percolation chain. OSLOM [10], starts with each node as the initial seed and optimizes a fitness function, defined as the probability of finding the cluster in a random

null model, to join together small clusters into statistically significant larger clusters. Seed Set Expansion (SSE) [11], [28] identifies overlapping communities by expanding different types of seeds by a personalized PageRank diffusion. DEMON [22] and another independent work in [29] identify very small, tightly connected sub-communities, create a new network in which each node represents such a sub-community, and then identify communities in this meta-network. Using spectral algorithms, Newman studies the three related problems of detection by modularity maximization, statistical inference or normalized-cut graph partitioning, and finds that with certain choices of the free parameters in these spectral algorithms the algorithms for all three problems are identical [30].

Local seed set expansion. Random walks have been extensively adopted as a subroutine for locally expanding the seed set [31], and this approach is observed to produce communities correlated highly to the ground-truth communities in real-world networks [32]. PageRank, heat kernel and local spectral diffusions are three main techniques for probability diffusion.

Spielman and Teng use degree-normalized personalized [33] PageRank (DN PageRank) with truncation of small values to expand a starting seed. DN PageRank has been used in several subsequent PageRank-based clustering algorithms [3], [31], including the popular PageRank Nibble method [13]. However, a study evaluating different variations of PageRank finds that standard PageRank yields better performance than DN PageRank [4].

The heat kernel method provides another local graph diffusion. Based on a continuous-time Markov chain, the heat kernel diffusion involves the exponential of a generator matrix, which may be approximated via a series expansion. Chung and collaborators have proposed a local graph partitioning based on the heat kernel diffusion [34], [35], and a Monte Carlo algorithm to estimate the heat kernel [14]. Another approach was described in [12], where the authors estimate the heat kernel diffusion via coordinate relaxation on an implicit linear system; their approach uncovers smaller communities with substantially higher F_1 measures than those found through the personalized PageRank diffusion.

Spectral methods are often used to extract disjoint communities from a few leading eigenvectors of a graph Laplacian [36], [37]. Recently, there has been a growing interest in adapting the spectral approach to mine the local structure around the seed set. Mahoney, Orecchia, and Vishnoi [23] introduce a locally-biased analogue of the second eigenvector for extracting local properties of data graphs near an input seed set by finding a sparse cut, and apply the method to semi-supervised image segmentation and local community extraction. In [15], [16], the authors introduce an algorithm to extract the local community by seeking a sparse vector from the local spectral subspaces using ℓ_1 norm optimization. They apply a power method for the subspace iteration using a standard random walk on a modified graph with a self loop on each node, which we call the light lazy random walk. They also apply a reseeding iteration to improve the detection accuracy.

Bounding the local community. All seed set expansion methods need a stopping criterion, unless the size of the target community is known in advance. Conductance is

commonly recognized as the best stopping criterion [3], [11], [12], [28]. Yang and Leskovec [3] provide widely-used real-world datasets with labeled ground truth, and find that conductance and triad-partition-ratio (TPR) are the two stopping rules yielding the highest detection accuracy. He et al. [15] propose two new metrics, TPN and nMod, and compare them with conductance, modularity and TPR; and they show that conductance and TPN consistently outperform other metrics. Laarhoven and Marchiori [6] study a continuous relaxation of conductance by investigating the relation of conductance with weighted kernel k -means.

Local seeding strategies. The seeding strategy is a key part of seed set expansion algorithms. Kloumann and Kleinberg [4] argue that random seeds are superior to high degree seeds, and suggest domain experts provide seeds with a diverse degree distribution. In the original LOSP paper [15], the authors compare low degree, random, high triangle participation (number of triangles inside the community containing the seed) and low escape seeds (judged by probability retained on the seeds after short random walks), and find all four types of seeds yield almost the same accuracy. They show that low degree seeds spread out the probabilities slowly and better preserve the local information, and random seeds are similar to low degree seeds due to the power law degree distribution. High triangle participation seeds and low escape seeds follow another philosophy: they choose seeds more cohesive to the target community.

3 PRELIMINARIES

3.1 Problem Formulation

The local community detection problem can be formalized as follows. We are given a connected, undirected graph $G = (V, E)$ with n nodes and m edges. Let $\mathbf{A} \in \{0, 1\}^{n \times n}$ be the associated adjacency matrix, \mathbf{I} the identity matrix, and \mathbf{e} the vector of all ones. Let $\mathbf{d} = \mathbf{A}\mathbf{e}$ be the vector of node degrees, and $\mathbf{D} = \text{diag}(\mathbf{d})$ the diagonal matrix of node degrees. Let S be the set of a few exemplary members in the target community $T = (V_t, E_t)$ ($S \subseteq V_t \subseteq V$, $|V_t| \ll |V|$). And let $s \in \{0, 1\}^n$ be a binary indicator vector representing the exemplary members in S . We are asked to identify the remaining latent members in the target community T .

3.2 Datasets

We consider four groups with a total of 28 synthetic datasets, five SNAP datasets in social, product, and collaboration domains, and three biology networks for a comprehensive evaluation on the proposed LOSP algorithms.

3.2.1 LFR Benchmark

For synthetic datasets, we use the LFR standard benchmark networks proposed by Lancichinetti et al. [38], [39]. The LFR benchmark graphs have a built-in community structure that simulates properties of real-world networks accounting for heterogeneity of node degrees and community sizes that follow power law distribution.

We adopt the same set of parameter settings used in [21] and generate four groups with a total of 28 LFR benchmark graphs. Table 1 summarizes the parameter settings we used, among which the mixing parameter μ has a big impact on

the network topology. μ controls the average fraction of neighboring nodes that do not belong to any community for each node, two ranges of typical community size, big and small, are provided by b and s . Each node belongs to either one community or om overlapping communities, and the number of nodes in overlapping communities is specified by on . A larger om or on indicates more overlaps that are harder for the community detection task.

For four groups of configurations based on the community size and on , we vary om from 2 to 8 to get seven networks in each group, denoted as:

- 1) **LFR_s_0.1** for $\{s : [10, 50], on = 500\}$;
- 2) **LFR_s_0.5** for $\{s : [10, 50], on = 2500\}$;
- 3) **LFR_b_0.1** for $\{b : [20, 100], on = 500\}$;
- 4) **LFR_b_0.5** for $\{b : [20, 100], on = 2500\}$.

3.2.2 Real-world Networks

We consider five real-world network datasets with labeled ground truth from the Stanford Network Analysis Project (SNAP)¹ and three genetic networks with labeled ground truth from the Isobase website².

- **SNAP:** The five SNAP networks, **Amazon**, **DBLP**, **LiveJ**, **YouTube**, **Orkut**, are in the domains of social, product, and collaboration [3]. For each network, we adopt the top 5000 annotated communities with the highest quality evaluated with several metrics by [3].
- **Isobase:** The three genetic networks from the Isobase website describe protein interactions. **HS** describes these interactions in humans, **SC** in *S. cerevisiae*, a type of yeast, and **DM** in *D. melanogaster*, a type of fruit fly. Such networks are interesting as communities may correspond to different genetic functions.

Table 2 summarizes the networks and their ground truth communities. We calculate the average and standard deviation of the community sizes, and the average conductance, where low conductance gives priority to communities with dense internal links and sparse external links. We also define and calculate the roundness of communities.

Definition 1. Roundness of a subgraph. The roundness of a subgraph $G' = (V', E')$ is the average shortest path among all pair-wise nodes divided by the longest shortest path in the subgraph.

The roundness value R is 1 for a clique, and $R = \frac{|V'|+1}{3(|V'|-1)} \approx \frac{1}{3}$ if the subgraph is a straight line. Because large roundness value indicates a “round” subgraph and small roundness value indicates a “long and narrow” subgraph, the roundness reveals some information on the topology structure of the subgraph. Table 2 shows that communities in the above real-world networks have an average roundness of about 0.67. If we normalize the roundness value from $[1/3, 1]$ to $[0, 1]$, then we get $R_{norm} = \frac{R-1/3}{1-1/3}$.

3.3 Evaluation Metric

For the evaluation metric, we adopt F_1 score to quantify the similarity between the detected local community C and

1. <http://snap.stanford.edu>
 2. <http://groups.csail.mit.edu/cb/mna/isobase/>

the target ground truth community T . The F_1 score for each pair of (C, T) is defined by:

$$F_1(C, T) = \frac{2 \cdot P(C, T) \cdot R(C, T)}{P(C, T) + R(C, T)},$$

where the precision P and recall R are defined as:

$$P(C, T) = \frac{|C \cap T|}{|C|}, R(C, T) = \frac{|C \cap T|}{|T|}.$$

TABLE 1
Parameters for the LFR benchmarks.

Parameter	Description
$n = 5000$	number of nodes in the graph
$\mu = 0.3$	mixing parameter
$\bar{d} = 10$	average degree of the nodes
$d_{max} = 50$	maximum degree of the nodes
$s : [10, 50], b : [20, 100]$	range of the community size
$\tau_1 = 2$	node degree distribution exponent
$\tau_2 = 1$	community size distribution exponent
$om \in \{2, 3, \dots, 8\}$	overlapping membership
$on \in \{500, 2500\}$	number of overlapping nodes

4 KRYLOV SUBSPACE CLUSTERING

It is well known that there is a close relationship between the combinatorial characteristics of a graph and the algebraic properties of its associated matrices [40]. In this section, we present a local community detection method of finding a linear sparse coding on the Krylov subspace, which is a local approximation of the spectral subspace. We first present the local sampling method starting from the seeds to reach a comparatively small subgraph G_s , and provide the theoretical base that finding a local community containing the seeds corresponds to finding a sparse linear coding in the invariant subspace spanned by the dominant eigenvectors of the transition matrix. Then we propose a family of the local spectral subspace definitions based on various short random walk diffusions, and do local community detection by finding a sparse relaxed indicator vector that lies in a local spectral subspace representing the subordinate probability of the corresponding nodes.

4.1 Local Sampling

We first do a local sampling from the seeds for large networks to reduce the computational complexity. According to the small world phenomenon and “six degrees of separation”, most members should be at most two or three steps far away from the seed members if we want to identify a small community of size hundreds. We mainly use Breadth-First Search (BFS) and filter some very popular nodes during the BFS expansion.

Starting from each seed, we do a one-step BFS. If the sampled subgraph is no greater than the lower bound N_1 , then we do one more round of BFS to contain more neighbor nodes. To avoid the second BFS expanding too many nodes, we first filter low inward frontier nodes (evaluated by the fraction of inward edges to the BFS subgraph) which may contain some inactive nodes or very popular nodes. The $\text{Filter}(\cdot)$ operation chooses high inward ratio nodes until

Algorithm 1 Sampling

Input: Graph $G = (V, E)$, seed set $S \subseteq V$, lower bound of sampled size from each seed N_1 , upper bound of the subgraph size N_2 , and steps of random walks k for postprocessing

Output: Sampled subgraph $G_s = (V_s, E_s)$

```

1:  $V_s \leftarrow S$ 
2: for each  $s_i \in S$  do
3:    $V_i \leftarrow \text{BFS}(s_i)$ 
4:    $V'_i \leftarrow V_i$ 
5:   while ( $|V_i| < N_1$ , BFS steps  $\leq 2$ ) do
6:      $V'_i \leftarrow \text{Filter}(V'_i)$ 
7:      $V'_i \leftarrow \text{BFS}(V'_i)$ 
8:      $V_i = V_i \cup V'_i$ 
9:   end while
10:   $V_s = V_s \cup V_i$ 
11: end for
12: if  $|V_s| > N_2$  then
13:   Conduct a  $k$ -steps of random walk from  $S$  in  $G_s$ 
14:    $V_s \leftarrow N_2$  nodes with higher probability
15: end if
16:  $G_s = (V_s, E_s)$  is the induced subgraph from  $V_s$ 

```

the total out-degree is no less than 3000. In the end, we union all BFS subgraphs obtained from each seed. If the amalgamated subgraph scale is larger than the upper bound N_2 , we then conduct a k -step short random walk from the seeds to remove some low probability nodes. Details of the sampling are as shown in Algorithm 1.

For the parameters, we empirically set $(N_1, N_2, k) = (300, 5000, 3)$ such that the resulting subgraph is large enough to cover almost all the members in the target community. Denote the sampled subgraph as $G_s = (V_s, E_s)$ with n_s nodes and m_s edges in the following discussion. We then identify the local community from this comparatively small subgraph instead of the original large network. The complexity is only related to the degrees of the nodes and it is very quick in seconds for the datasets we considered. The sampling quality, evaluated by the coverage ratio of the labeled nodes, plays a key role for the follow-up membership identification. And this pre-processing procedure significantly reduces the membership identification cost.

4.2 Spectra and Local Community

In this subsection, we provide the necessary theoretical base that finding a low-conductance community corresponds to finding a sparse indicator vector in the span of dominant eigenvectors of the transition matrix with larger eigenvalues.

Let $\mathbf{L} = \mathbf{D}_s - \mathbf{A}_s$ be the Laplacian matrix of G_s where \mathbf{A}_s and \mathbf{D}_s denote the adjacency matrix and the diagonal degree matrix of G_s . We define two normalized graph Laplacian matrices:

$\mathbf{L}_{rw} = \mathbf{I} - \mathbf{N}_{rw} = \mathbf{D}_s^{-1} \mathbf{L}$, $\mathbf{L}_{sym} = \mathbf{I} - \mathbf{N}_{sym} = \mathbf{D}_s^{-\frac{1}{2}} \mathbf{L} \mathbf{D}_s^{-\frac{1}{2}}$, where $\mathbf{N}_{rw} = \mathbf{D}_s^{-1} \mathbf{A}_s$ is the transition matrix, and $\mathbf{N}_{sym} = \mathbf{D}_s^{-\frac{1}{2}} \mathbf{A}_s \mathbf{D}_s^{-\frac{1}{2}}$ is the normalized adjacency matrix.

TABLE 2
Statistics for real-world networks and their ground truth communities.

Domain	Network			Ground truth communities			
	Name	# Nodes	# Edges	Avg. \pm Std. Size	Avg. Cond.	Roundness R	R_{norm}
Product	Amazon	334,863	925,872	13 \pm 18	0.07	0.69	0.54
Collaboration	DBLP	317,080	1,049,866	22 \pm 201	0.41	0.74	0.61
Social	LiveJ	3,997,962	34,681,189	28 \pm 58	0.39	0.65	0.48
Social	YouTube	1,134,890	2,987,624	21 \pm 73	0.84	0.69	0.54
Social	Orkut	3,072,441	117,185,083	216 \pm 321	0.73	-	-
Biology	DM	15,294	485,408	440 \pm 2096	0.88	0.68	0.52
Biology	HS	10,153	54,570	113 \pm 412	0.88	0.58	0.37
Biology	SC	5,523	82,656	67 \pm 110	0.90	0.63	0.45

For a community C , the conductance [18] of C is defined as

$$\Phi(C) = \frac{\text{cut}(C, \bar{C})}{\min\{\text{vol}(C), \text{vol}(\bar{C})\}},$$

where \bar{C} consists of all nodes outside C , $\text{cut}(C, \bar{C})$ denotes the number of edges between, and $\text{vol}(\cdot)$ calculates the "edge volume", i.e. for the subset nodes, we count their total node degrees in graph G_s . Low conductance gives priority to a community with dense internal links and sparse external links.

Let $\mathbf{y} \in \{0, 1\}^{n_s}$ be a binary indicator vector representing a small community C in the sampled graph G_s . As $\mathbf{y}^T \mathbf{D}_s \mathbf{y}$ equals the total node degrees of C , and $\mathbf{y}^T \mathbf{A}_s \mathbf{y}$ equals two times the number of internal edges of C , the conductance $\Phi(C)$ could be written as a generalized Rayleigh quotient

$$\Phi(C) = \frac{\mathbf{y}^T \mathbf{L}_s \mathbf{y}}{\mathbf{y}^T \mathbf{D}_s \mathbf{y}} = \frac{(\mathbf{D}_s^{\frac{1}{2}} \mathbf{y})^T \mathbf{L}_{\text{sym}} (\mathbf{D}_s^{\frac{1}{2}} \mathbf{y})}{(\mathbf{D}_s^{\frac{1}{2}} \mathbf{y})^T (\mathbf{D}_s^{\frac{1}{2}} \mathbf{y})}.$$

Let $\mathbf{L}_{\text{sym}} = \mathbf{Q} \mathbf{\Lambda} \mathbf{Q}^T$ be the eigendecomposition, where $\mathbf{Q} = [\mathbf{q}_1 | \dots | \mathbf{q}_{n_s}]$ is an orthonormal matrix and $\mathbf{\Lambda} = \text{diag}(\lambda_1, \dots, \lambda_{n_s})$, $\lambda_1 \leq \dots \leq \lambda_{n_s}$. Then

$$\Phi(C) = \frac{(\mathbf{Q}^T \mathbf{D}_s^{\frac{1}{2}} \mathbf{y})^T \mathbf{\Lambda} (\mathbf{Q}^T \mathbf{D}_s^{\frac{1}{2}} \mathbf{y})}{(\mathbf{Q}^T \mathbf{D}_s^{\frac{1}{2}} \mathbf{y})^T (\mathbf{Q}^T \mathbf{D}_s^{\frac{1}{2}} \mathbf{y})}.$$

Let $x_i = \mathbf{q}_i^T \mathbf{D}_s^{\frac{1}{2}} \mathbf{y}$ be the projection of $\mathbf{D}_s^{\frac{1}{2}} \mathbf{y}$ on the i th eigenvector \mathbf{q}_i of \mathbf{L}_{sym} , we have

$$\Phi(C) = \frac{\sum_{i=1}^{n_s} \lambda_i x_i^2}{\sum_{i=1}^{n_s} x_i^2} = \sum_{i=1}^{n_s} w_i \lambda_i, \quad (1)$$

where $w_i = \frac{x_i^2}{\sum_{i=1}^{n_s} x_i^2}$ is the weighting coefficient of the eigenvalues. If $\Phi(C)$ is close to the smallest eigenvalue λ_1 , then most of the weight on average must be on the eigenvalues close to λ_1 .

Theorem 1. Let ϵ be a small positive real number, if $\Phi(C) < \lambda_1 + \epsilon$, then for any positive real number t ,

$$\sum_{i: \lambda_i < \lambda_1 + t\epsilon} w_i > 1 - \frac{1}{t}$$

Proof: By Eq. (1) we have

$$\begin{aligned} \Phi(C) &= \sum_{i: \lambda_i < \lambda_1 + t\epsilon} w_i \lambda_i + \sum_{j: \lambda_j \geq \lambda_1 + t\epsilon} w_j \lambda_j \\ &\geq \lambda_1 \sum_{i: \lambda_i < \lambda_1 + t\epsilon} w_i + (\lambda_1 + t\epsilon) \sum_{j: \lambda_j \geq \lambda_1 + t\epsilon} w_j \\ &= \lambda_1 + t\epsilon \sum_{j: \lambda_j \geq \lambda_1 + t\epsilon} w_j. \end{aligned}$$

As $\Phi(C) < \lambda_1 + \epsilon$, we get

$$\lambda_1 + t\epsilon \sum_{j: \lambda_j \geq \lambda_1 + t\epsilon} w_j < \lambda_1 + \epsilon.$$

Therefore,

$$\sum_{j: \lambda_j \geq \lambda_1 + t\epsilon} w_j < \frac{1}{t}, \quad \sum_{i: \lambda_i < \lambda_1 + t\epsilon} w_i > 1 - \frac{1}{t}.$$

□

Theorem 1 indicates for a low conductance $\Phi(C)$ close to the smallest value λ_1 , the smaller eigenvalues of \mathbf{L}_{sym} contribute most of the weights. Relax $\mathbf{y} \in [0, 1]^{n_s}$, as $w_i = \frac{x_i^2}{\sum_{i=1}^{n_s} x_i^2}$ and $x_i = \mathbf{q}_i^T \mathbf{D}_s^{\frac{1}{2}} \mathbf{y}$, the relaxed scaled indicator vector $\mathbf{D}_s^{\frac{1}{2}} \mathbf{y}$ should be well approximated by a linear combination of the dominant eigenvectors with smaller eigenvalues. As

$$\mathbf{L}_{\text{rw}} \mathbf{v} = \lambda \mathbf{v} \Leftrightarrow \mathbf{L}_{\text{sym}} (\mathbf{D}_s^{\frac{1}{2}} \mathbf{v}) = \lambda (\mathbf{D}_s^{\frac{1}{2}} \mathbf{v}),$$

where \mathbf{v} is a nonzero vector. It shows that the relaxed indicator vector \mathbf{y} should be well approximated by a linear combination of the dominant eigenvectors of \mathbf{L}_{rw} with smaller eigenvalues. Also,

$$\mathbf{L}_{\text{rw}} \mathbf{v} = (\mathbf{I} - \mathbf{N}_{\text{rw}}) \mathbf{v} = \lambda \mathbf{v} \Leftrightarrow \mathbf{N}_{\text{rw}} \mathbf{v} = (1 - \lambda) \mathbf{v},$$

it follows that \mathbf{L}_{rw} and \mathbf{N}_{rw} share the same set of eigenvectors and the corresponding eigenvalue of \mathbf{N}_{rw} is $1 - \lambda$ where λ is the eigenvalue of \mathbf{L}_{rw} . Equivalently, the relaxed indicator vector \mathbf{y} should be well approximated by a linear combination of the eigenvectors of \mathbf{N}_{rw} with larger eigenvalues.

This leads to our idea of finding a relaxed sparse indicator vector \mathbf{y} containing the seeds in the span of the dominant eigenvectors with larger eigenvalues of \mathbf{N}_{rw} :

$$\begin{aligned} \min \quad & \|\mathbf{y}\|_1 = \mathbf{e}^T \mathbf{y} \\ \text{s.t.} \quad & (1) \mathbf{y} = \mathbf{V}_d \mathbf{x}, \\ & (2) y_i \in [0, 1], \\ & (3) y_i \geq \frac{1}{|S|}, i \in S, \end{aligned} \quad (2)$$

where the column vectors of \mathbf{V}_d are formed by the dominant eigenvectors of \mathbf{N}_{rw} with larger values and \mathbf{e} is the vector of all ones. \mathbf{x} is the coefficient vector, and y_i denotes the i th element of the binary indicator vector \mathbf{y} . $\mathbf{y} = \mathbf{V}_d \mathbf{x}$ indicates that \mathbf{y} lies in the eigenspace spanned by the column vectors of \mathbf{V}_d . \mathbf{y} indicates the local community with low conductance containing the labeled seeds. Section 4.5 provides detailed analysis on the bounding performance for the conductance of the local community.

4.3 Krylov Subspace Approximation

4.3.1 Variants of Random Walk Diffusion

Instead of using the eigenvalue decomposition on \mathbf{N}_{rw} , we consider short random walks for the probability diffusion starting from the seed set to get the “local spectral subspace”. We define several variants of the spectral diffusion based on different transition matrices for the random walks.

1) *Standard Random Walk* uses the transition matrix \mathbf{N}_{rw} for the probability diffusion.

$$\mathbf{N}_{\text{rw}} = \mathbf{D}_s^{-1} \mathbf{A}_s. \quad (3)$$

2) *Light Lazy Random Walk* retains some probability at the current node for the random walks.

$$\mathbf{N}_{\text{rw}} = (\mathbf{D}_s + \alpha \mathbf{I})^{-1} (\alpha \mathbf{I} + \mathbf{A}_s), \quad (4)$$

where $\alpha \in N^{0+}$. $\alpha = 0$ degenerates to the standard random walk and $\alpha = 1, 2, 3, \dots$ corresponds to a random walk in the modified graph with 1, 2, 3, ... loops at each node.

3) *Lazy Random Walk* is defined by

$$\begin{aligned} \mathbf{N}_{\text{rw}} &= (\mathbf{D}_s + \alpha \mathbf{D}_s)^{-1} (\alpha \mathbf{D}_s + \mathbf{A}_s) \\ &= \frac{\alpha}{1 + \alpha} \mathbf{I} + \frac{1}{1 + \alpha} \mathbf{D}_s^{-1} \mathbf{A}_s, \end{aligned} \quad (5)$$

where $\alpha \in [0, 1]$. E.g. $\alpha = 0.1$ corresponds to a random walk that always retains $\frac{0.1}{1+0.1}$ probability on the current node during the diffusion process. $\alpha = 0$ degenerates to the standard random walk.

4) *Personalized PageRank (PPR)* is defined by

$$\mathbf{N}_{\text{rw}} = \alpha \mathbf{S} + (1 - \alpha) \mathbf{D}_s^{-1} \mathbf{A}_s, \quad (6)$$

where $\alpha \in [0, 1]$ and \mathbf{S} the diagonal matrix with binary indicators for the seed set S . E.g. $\alpha = 0.1$ corresponds to a random walk that always retains 10% of the probability on the seed set. $\alpha = 0$ is the standard random walk.

4.3.2 Regular or Inverse Random Walks

Based on the above random walk diffusion definition, one step of random walk is defined as $\mathbf{N}_{\text{rw}}^T \mathbf{p}$ for a probability column vector \mathbf{p} , and the probability density for a random walk of length k is given by a Markov chain:

$$\mathbf{p}_k = \mathbf{N}_{\text{rw}}^T \mathbf{p}_{k-1} = (\mathbf{N}_{\text{rw}}^T)^k \mathbf{p}_0, \quad (7)$$

where \mathbf{p}_0 is the initial probability density evenly assigned on the seeds.

We can also define an “inverse random walk”:

$$\mathbf{p}_k = \mathbf{N}_{\text{rw}} \mathbf{p}_{k-1} = (\mathbf{N}_{\text{rw}})^k \mathbf{p}_0. \quad (8)$$

Here \mathbf{p}_k indicates a probability density such that the probability concentrates to the seed set as \mathbf{p}_0 after k steps of short random walks. The value of \mathbf{p}_k also shows a snapshot of the probability distribution for the local community around the seed set, and follow-up experiments also demonstrates the effectiveness of the “inverse random walk”, which has a slightly lower accuracy as compared with the “regular random walk”.

4.3.3 Local Spectral Subspace

Then we define a local spectral subspace as a proxy of the invariant subspace spanned by the leading eigenvectors of \mathbf{N}_{rw} . The local spectral subspace is defined on an order- d Krylov matrix and k is the number of diffusion steps:

$$\mathbf{V}_d^{(k)} = [\mathbf{p}_k, \mathbf{p}_{k+1}, \dots, \mathbf{p}_{k+d-1}]. \quad (9)$$

Here k and d are both some modest numbers. Then the Krylov subspace spanned by the column vectors of $\mathbf{V}_d^{(k)}$ is called the local spectral subspace. As $k \rightarrow \infty$, the local spectral subspace built on “regular random walk” approaches

the eigenspace associated with d left eigenvectors of \mathbf{N}_{rw} with larger eigenvalues, and the local spectral subspace built on “inverse random walk” approaches the eigenspace associated with d right eigenvectors of \mathbf{N}_{rw} with larger eigenvalues. Our interest now, though, is not in the limiting case when k is large, but for a much more modest number of diffusion steps. Based on different local spectral diffusions in Eq. (3) - Eq. (6), we have a set of local spectral subspace definitions. Based on Eq. (7) or Eq. (8), we have two sets of local spectral subspace definitions.

Experiments in Section 5 show that the definitions on \mathbf{N}_{rw}^T , which is on the regular random walk, is considerably better than that on \mathbf{N}_{rw} for the detection accuracy. However, the definitions on \mathbf{N}_{rw} corresponding to the inverse random walk also show high accuracy as compared with the baselines. Our results show that the local approximation built on “regular random walk” show higher accuracy than that built on “inverse random walk”.

4.4 Local Community Detection

We modify the optimization problem shown in Eq. (2) by relaxing each element in the indicator vector \mathbf{y} to be non-negative, and approximating the global spectral subspace by the local spectral subspace. Thus, we seek a relaxed sparse vector in the local spectral subspace by solving a linear programming problem:

$$\begin{aligned} \min \quad & \|\mathbf{y}\|_1 = \mathbf{e}^T \mathbf{y} \\ \text{s.t.} \quad & (1) \mathbf{y} = \mathbf{V}_d^{(k)} \mathbf{x}, \\ & (2) \mathbf{y} \geq 0, \\ & (3) y_i \geq \frac{1}{|S|}, i \in S. \end{aligned} \quad (10)$$

This is an ℓ_1 norm approximation for finding a sparse linear coding that indicates a small community containing the seeds with \mathbf{y} in the local spectral subspace spanned by the column vectors of $\mathbf{V}_d^{(k)}$. y_i indicates the belonging likelihood of node i in the target community.

1) If $|V_t|$ is known, we then sort the values in \mathbf{y} in non-ascending order and select the corresponding $|V_t|$ nodes with the higher belonging likelihood as the output community. Denote the corresponding local community detection methods based on Eq. (3) - Eq. (6) as: LRw (LOSP based on Random Weight), LLi (LOSP based on Light Lazy Random Weight), LLa (LOSP based on Lazy Random Weight) and LPr (LOSP based on PPR).

2) If $|V_t|$ is unknown, we use a heuristic to determine the community boundary. We sort the nodes based on the element values of \mathbf{y} in the decreasing order, and find a set S_{k^*} with the first k^* nodes having a comparatively low conductance. Specifically, we start from an index k_0 where set S_{k_0} contains all the seeds. We then generate a sweep curve $\Phi(S_k)$ by increasing index k . Let k^* be the value of k where $\Phi(S_k)$ achieves a first local minimum. The set S_{k^*} is regarded as the detected community.

We determine a local minima as follows. If at some point k^* when we are increasing k , $\Phi(S_k)$ stops decreasing, then this k^* is a candidate point for the local minimum. If $\Phi(S_k)$ keeps increasing after k^* and eventually becomes higher than $\alpha \Phi(S_{k^*})$, then we take k^* as a valid local minimum.

We experimented with several values of α on a small trial of data and found that $\alpha = 1.02$ gives good performance across all the datasets.

4.5 Bounding Analysis

In the following discussion, we provide analysis to relate spectral properties to the conductance, and give the bounding performance on the conductance value.

Theorem 2. (Courant-Fischer Formula) Let \mathbf{H} be an $n \times n$ symmetric matrix with eigenvalues $\lambda_1^{(\mathbf{H})} \leq \lambda_2^{(\mathbf{H})} \leq \dots \leq \lambda_n^{(\mathbf{H})}$ and corresponding eigenvectors $\mathbf{v}_1, \dots, \mathbf{v}_n$. Then

$$\begin{aligned}\lambda_1^{(\mathbf{H})} &= \min_{\|\mathbf{x}\|_2=1} \mathbf{x}^T \mathbf{H} \mathbf{x} = \min_{\mathbf{x} \neq \mathbf{0}} \frac{\mathbf{x}^T \mathbf{H} \mathbf{x}}{\mathbf{x}^T \mathbf{x}}, \\ \lambda_2^{(\mathbf{H})} &= \min_{\substack{\|\mathbf{x}\|_2=1 \\ \mathbf{x} \perp \mathbf{v}_1}} \mathbf{x}^T \mathbf{H} \mathbf{x} = \min_{\substack{\mathbf{x} \neq \mathbf{0} \\ \mathbf{x} \perp \mathbf{v}_1}} \frac{\mathbf{x}^T \mathbf{H} \mathbf{x}}{\mathbf{x}^T \mathbf{x}}, \\ \lambda_n^{(\mathbf{H})} &= \max_{\|\mathbf{x}\|_2=1} \mathbf{x}^T \mathbf{H} \mathbf{x} = \max_{\mathbf{x} \neq \mathbf{0}} \frac{\mathbf{x}^T \mathbf{H} \mathbf{x}}{\mathbf{x}^T \mathbf{x}}.\end{aligned}$$

We will not include the proof of the Courant-Fischer Formula here. The interested reader is referred to [41].

Let \mathbf{L}_{sym} be the normalized graph Laplacian matrix of G_s with eigenvalues $\lambda_1 \leq \dots \leq \lambda_{n_s}$ and corresponding eigenvectors $\mathbf{q}_1, \dots, \mathbf{q}_{n_s}$. As $\mathbf{L}_{\text{sym}}(\mathbf{D}_s^{-\frac{1}{2}} \mathbf{e}) = \mathbf{0}$ where \mathbf{e} is the vector of all ones, we have $\lambda_1 = 0$, $\mathbf{q}_1 = \frac{\mathbf{D}_s^{-\frac{1}{2}} \mathbf{e}}{\|\mathbf{D}_s^{-\frac{1}{2}} \mathbf{e}\|_2}$.

By the Courant-Fischer Formula, we have

$$\begin{aligned}\lambda_2 &= \min_{\substack{\mathbf{x} \neq \mathbf{0} \\ \mathbf{x} \perp \mathbf{q}_1}} \frac{\mathbf{x}^T \mathbf{L}_{\text{sym}} \mathbf{x}}{\mathbf{x}^T \mathbf{x}} = \min_{\substack{\mathbf{z} \neq \mathbf{0} \\ \mathbf{z} \perp \mathbf{D}_s \mathbf{e}}} \frac{\mathbf{z}^T \mathbf{L} \mathbf{z}}{\mathbf{z}^T \mathbf{D}_s \mathbf{z}} \\ &= \min_{\substack{\mathbf{z} \neq \mathbf{0} \\ \mathbf{z} \perp \mathbf{D}_s \mathbf{e}}} \frac{\sum_{i \sim j} (z_i - z_j)^2}{\sum_i d_i z_i^2},\end{aligned}\quad (11)$$

where $\mathbf{z} = \mathbf{D}_s^{-\frac{1}{2}} \mathbf{x}$, d_i is the degree of the i th node and $\sum_{i \sim j}$ denotes the sum over all unordered pairs $\{i, j\}$ for which i and j are adjacent.

Theorem 3. The conductance $\Phi(C)$ of a small community $C = (V_c, E_c)$ in graph G_s ("small" means $\text{vol}(C) \leq 0.5 \text{vol}(G_s)$) is bounded by

$$\frac{\lambda_2}{2} \leq \Phi(C) \leq 1,$$

where $\text{vol}(A)$ denotes for all nodes inside $A \subseteq V_s$, we count the total degree in graph G_s .

Proof: Let $\mathbf{z} = \mathbf{y} - \sigma \mathbf{e}$, where $\mathbf{y} \in \{0, 1\}^{n_s}$ is a binary indicator vector representing community C in graph G_s , \mathbf{e} the vector of all ones, and $\sigma = \frac{\text{vol}(C)}{\text{vol}(G_s)}$.

We can check that $\mathbf{z} \perp \mathbf{D}_s \mathbf{e}$:

$$\begin{aligned}\mathbf{z}^T \mathbf{D}_s \mathbf{e} &= \mathbf{y}^T \mathbf{D}_s \mathbf{e} - \sigma \mathbf{e}^T \mathbf{D}_s \mathbf{e} \\ &= \text{vol}(C) - \frac{\text{vol}(C)}{\text{vol}(G_s)} \text{vol}(G_s) = 0.\end{aligned}$$

We also know

$$\mathbf{z}^T \mathbf{L} \mathbf{z} = (\mathbf{y} - \sigma \mathbf{e})^T \mathbf{L} (\mathbf{y} - \sigma \mathbf{e}) = \mathbf{y}^T \mathbf{L} \mathbf{y}.$$

It remains to compute

$$\begin{aligned}\mathbf{z}^T \mathbf{D}_s \mathbf{z} &= (\mathbf{y} - \sigma \mathbf{e})^T \mathbf{D}_s (\mathbf{y} - \sigma \mathbf{e}) \\ &= \mathbf{y}^T \mathbf{D}_s \mathbf{y} - 2\sigma \mathbf{y}^T \mathbf{D}_s \mathbf{e} + \sigma^2 \mathbf{e}^T \mathbf{D}_s \mathbf{e} \\ &= \text{vol}(C) - 2\sigma \text{vol}(C) + \sigma^2 \text{vol}(G_s) \\ &= \frac{\text{vol}(C) \text{vol}(G_s - C)}{\text{vol}(G_s)}.\end{aligned}$$

By Eq. (11), we have

$$\lambda_2 \leq \frac{\mathbf{z}^T \mathbf{L} \mathbf{z}}{\mathbf{z}^T \mathbf{D}_s \mathbf{z}} = \frac{\mathbf{y}^T \mathbf{L} \mathbf{y} \cdot \text{vol}(G_s)}{\text{vol}(C) \text{vol}(G_s - C)}. \quad (12)$$

As the larger value of $\text{vol}(C)$ and $\text{vol}(G_s - C)$ is at least half of $\text{vol}(G_s)$,

$$\begin{aligned}\lambda_2 &\leq 2 \frac{\mathbf{y}^T \mathbf{L} \mathbf{y}}{\min(\text{vol}(C), \text{vol}(G_s - C))} = 2 \frac{\mathbf{y}^T \mathbf{L} \mathbf{y}}{\text{vol}(C)} \\ &= 2 \frac{\mathbf{y}^T \mathbf{L} \mathbf{y}}{\mathbf{y}^T \mathbf{D}_s \mathbf{y}} = 2\Phi(C).\end{aligned}$$

Therefore,

$$\frac{\lambda_2}{2} \leq \Phi(C).$$

And it is obvious that

$$\Phi(C) = \frac{\mathbf{y}^T \mathbf{L} \mathbf{y}}{\mathbf{y}^T \mathbf{D}_s \mathbf{y}} \leq 1. \quad (13)$$

□

For a small community in a large network, for example the total degree of the small community is one tenth of the total degree of the graph, by Eq. (12) and (13), $0.9\lambda_2 \leq \Phi(C) \leq 1$. In the following, We provide a bounding analysis on λ_2 .

Definition 2 (Diameter of a graph). The diameter of a graph G , denoted by $D(G) = \max_{u,v} d(u, v)$, is the longest shortest path between any two nodes u, v in G .

Theorem 4. If G_s is a connected, undirected graph that contains $n_s \geq 2$ nodes, then

$$\frac{1}{D(G_s) \cdot \text{vol}(G_s)} \leq \lambda_2 \leq \frac{n_s}{n_s - 1}$$

Proof: Consider the trace of \mathbf{L}_{sym} , we have

$$\text{tr}(\mathbf{L}_{\text{sym}}) = \text{tr}(\mathbf{I}) - \text{tr}(\mathbf{D}_s^{-\frac{1}{2}} \mathbf{A}_s \mathbf{D}_s^{-\frac{1}{2}}) = n_s,$$

$$\text{tr}(\mathbf{L}_{\text{sym}}) = \sum_{i=1}^{n_s} \lambda_i = \sum_{i=2}^{n_s} \lambda_i \geq (n_s - 1)\lambda_2.$$

So $\lambda_2 \leq \frac{n_s}{n_s - 1}$. And by [40], we know $\lambda_2 \geq \frac{1}{D(G_s) \cdot \text{vol}(G_s)}$. □

Corollary 1. The conductance $\Phi(C)$ of a small community $C = (V_c, E_c)$ in connected graph G_s with diameter $D(G_s)$ is bounded by

$$\frac{1}{D(G_s) \cdot \text{vol}(G_s)} \leq \lambda_2 \leq \frac{n_s}{n_s - 1},$$

where $\text{vol}(G_s)$ denotes the total degrees of the sampled graph G_s .

5 EXPERIMENTS AND RESULTS

We implement the family of local spectral methods (LOSPs) in Matlab³ and thoroughly compare them with state-of-the-art localized community detection algorithms on the 28 LFR datasets as well as the 8 real-world networks across multiple domains. For the 5 SNAP datasets, we randomly locate 500 labeled ground truth communities on each dataset, and randomly pick three exemplary seeds from each target community. For the 28 LFR datasets and the 3 Biology datasets, we deal with every ground truth community and randomly pick three exemplary seeds from each ground truth community. We pre-process all real-world datasets by sampling, and apply the local spectral methods for each network.

3. <https://github.com/KunHe2015/LOSP/>

5.1 Statistics on Sampling

Table 3 provides statistics on real-world networks for the sampling method in Algorithm 1. The coverage indicates the average fraction of ground truth covered by the sampled subgraph, and n_s/n indicates the sampling rate which is the average fraction of subgraph size as compared with the original network scale.

For SNAP datasets, our sampling method has a high coverage with reasonable sample size, covering about 96% ground truth with a small average sampling rate of less than 0.1%, and the sampling procedure is within 14 seconds.

For the Biology networks, which are comparatively denser, the sampled subgraph covers about 91% ground truth with a relatively high sampling rate, and the sampling procedure is very fast in less than 0.2 seconds.

TABLE 3
Statistics on average values for the sampling on real-world networks.

	Networkx	Coverage	n_s	n_s/n	Time(s)
SNAP	Amazon	0.990	34	0.0001	0.730
	DBLP	0.980	198	0.0002	0.720
	LiveJ	1.000	629	0.0002	19.050
	YouTube	0.950	3237	0.0028	3.760
	Orkut	0.870	4035	0.0013	44.430
	Average	0.958	1627	0.0009	13.738
Biology	DM	0.910	2875	0.1880	0.256
	HS	0.876	2733	0.2692	0.125
	SC	0.947	3341	0.6049	0.076
	Average	0.911	2983	0.3540	0.152

5.2 Parameter Setup

To remove the impact of different local spectral methods in finding a local minimum for the community boundary, we use the ground truth size as a budget for parameter testing on the family of LOSP methods. When we say LOSP, we mean the family of LOSP defined on the N_{rw}^T Krylov subspace, which is the normal case for random walk diffusion. A comparison in Section 5.3 will show that in general, LOSP defined on N_{rw}^T Krylov subspace outperforms that on N_{rw} Krylov subspace with respect to the accurate detection.

Dimension of the subspace and diffusion steps. For local spectral subspace, we need to choose some modest numbers for the step k of random walks and the subspace dimension d such that the probability diffusion does not reach the global stationary. We did a small trial parameter study on all datasets, and found that $d = 2$ and $k = 2$ perform the best in general.

Parameters for the random walk diffusion. We thoroughly evaluate different spectral diffusion methods on all datasets, as shown in Fig. 1 and Fig. 2. The three columns correspond to light lazy random walk, lazy random walk and personalized pagerank with different α parameters. All three variants degenerate to the standard random walk when $\alpha = 0$. The results show that light lazy random walk, lazy random walk and personalized pagerank are robust for different α parameters. The personalized pagerank declines significantly when $\alpha = 1$ as all probability returns to the original seed set.

During the probability diffusion, light lazy random walk and lazy random walk always retain a ratio of probability

on the current set of nodes to keep the detected structure to be “local”. The personalized pagerank always returns a ratio of probability from the current nodes to the seed set. Instead of retaining some probability distribution on the current set of nodes, the personalized pagerank “shrinks” some probability to the original seed set. Such process also wants to keep the probability distribution “local” but it is not continuous as compared with the previous two methods.

In the following discussion, we set $\alpha = 1$ for light lazy random walk and lazy random walk, and set $\alpha = 0.1$ for personalized pagerank.

5.3 Evaluation on Local Spectral Methods

To remove the impact of different methods in finding a local minimum for the community boundary, we use the ground truth size as a budget for the proposed four LOSP variants: LRw (standard), LLi (light lazy), LLa (lazy) and LPr (pagerank). We first compare the four LOSP variants defined on the standard N_{rw}^T Krylov subspace, then compare the general performance on subspaces defined on either N_{rw}^T or N_{rw} .

Evaluation on variants of N_{rw}^T Krylov subspace. Fig. 3 illustrates the average detection accuracy on the eight real-world datasets. LRw, LLi, LLa and LPr achieve almost the same performance on almost all datasets. One exception is on YouTube that LLi, LLa and LPr considerably outperform LRw.

Fig. 4 illustrates the average detection accuracy on the four sets with a total of 28 LFR networks. For $\mu = 0.1$, Fig. 4 (a) and (c) show that LRw, LLi and LPr achieve almost the same performance and outperform LLa on average. For $\mu = 0.3$, Fig. 4 (b) and (d) show that LLi, LLa and LPr achieve almost the same performance and outperform LRw on average. On both cases, LLi and LPr, LOSP with light lazy or pagerank diffusion, demonstrate higher accuracy.

For the running time on the sampled subgraphs of all datasets, LRw, LLi, LLa and LPr take almost the same time of less than one second.

Comparison on N_{rw}^T or N_{rw} Krylov subspace. We compare the average F_1 score on each group of networks: SNAP, Biology and the four groups of LFR. Table 4 shows the comparison of detection accuracy where the community is truncated on truth size for subspace definitions on N_{rw}^T and N_{rw} respectively (The best three values on each row appear in bold). In general, N_{rw}^T outperforms N_{rw} , especially on real world datasets. When comparing with the LOSP variant defined on N_{rw} , the four variants defined on N_{rw}^T is about 15% or 5% higher F_1 scores on SNAP and Biology respectively. As for the synthetic LFR datasets, in general, N_{rw}^T performs slightly better than N_{rw} on the small ground truth communities, while N_{rw} performs slightly better than N_{rw}^T on the big ground truth communities. Among all the variants of LOSP, LLi on N_{rw}^T is always on top three for all datasets.

It is interesting that the results on N_{rw} is reasonably good, and even if we use the first local conductance to do the truncation, as shown in Table 5 (The best three values on each row appear in bold), the accuracy decays by about 5% to 15% as compared with that of the truncation on truth size, but it is still much better than the state-of-art

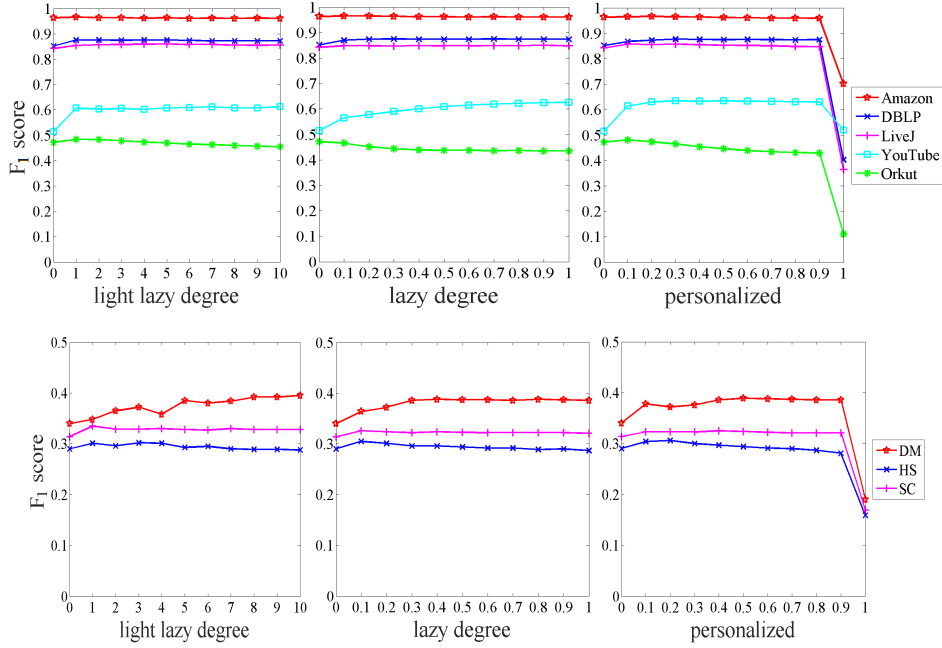


Fig. 1. Evaluation of different diffusion parameters on real-world datasets (Defined on N_{rw}^T , Krylov subspace, community size truncated by truth size). The three diffusions are robust for different α parameters, except for $\alpha = 1$ on personalized pagerank, in which case all probability returns to the original seed set.

TABLE 4
Comparison of average F_1 score for subspaces on N_{rw}^T or N_{rw} (Truncated on truth size).

Datasets	Subspace on N_{rw}^T				Subspace on N_{rw}			
	LRw	LLi	LLa	LPr	LRw	LLi	LLa	LPr
SNAP	0.729	0.757	0.749	0.757	0.556	0.578	0.594	0.601
Biology	0.315	0.328	0.331	0.335	0.266	0.287	0.246	0.284
LFR_s_0.1	0.660	0.675	0.570	0.677	0.628	0.673	0.600	0.660
LFR_s_0.5	0.341	0.381	0.356	0.371	0.317	0.373	0.364	0.351
LFR_b_0.1	0.515	0.536	0.488	0.526	0.523	0.568	0.516	0.550
LFR_b_0.5	0.238	0.273	0.265	0.260	0.230	0.272	0.272	0.254

TABLE 5
Comparison of average F_1 score for subspaces on N_{rw}^T or N_{rw} (Truncated on local minimal conductance).

Datasets	Subspace on N_{rw}^T				Subspace on N_{rw}			
	LRw	LLi	LLa	LPr	LRw	LLi	LLa	LPr
SNAP	0.593	0.620	0.599	0.604	0.503	0.518	0.526	0.514
Biology	0.150	0.182	0.206	0.171	0.135	0.146	0.166	0.160
LFR_s_0.1	0.554	0.574	0.443	0.561	0.539	0.576	0.518	0.546
LFR_s_0.5	0.232	0.334	0.265	0.291	0.217	0.332	0.337	0.311
LFR_b_0.1	0.358	0.387	0.296	0.365	0.393	0.406	0.353	0.348
LFR_b_0.5	0.134	0.198	0.168	0.169	0.131	0.217	0.214	0.186

local community detection algorithms, heat kernel(HK) and pagerank(PR), whose results are listed in Table 6 and Table 7, the average F_1 score on each dataset.

5.4 Final Comparison

For the final comparison, we find a local minimum of conductance to automatically determine the community boundary. We compare the family of LOSP defined on the N_{rw}^T Krylov subspace on all datasets with two state-of-the-art local community detection algorithms, HK for `hk-relax` [12] and PR for `pprpush` [13]. PR is based on the pagerank

diffusion while HK is based on heat kernel diffusion. To make a fair comparison, we run the six algorithms on the same three seeds randomly chosen from the ground truth communities.

5.4.1 Comparison on Real-world Datasets

For each of the real-world networks, Table 6 shows the average detection accuracy and conductance of the detected communities, Table 8 shows the average community size and running time.

For the SNAP datasets in product, collaboration and social domains, every variant of LOSP yields considerably higher accuracy on the first four datasets (Amazon, DBLP, LiveJ and Youtube), and yields slightly lower accuracy on Orkut. To have a better understanding on the results, we compare the property of the detection with the property of the ground truth communities, as shown in Table 2.

- For the first four datasets, the average size of the ground truth is small between 10 to 30, and the conductance is diverse (very low in Amazon and very high in YouTube). In general, the size and conductance of our detected communities are closest to the ground truth.
- For the last dataset Orkut, the size of ground truth is fairly large in 200, and the conductance is also high in 0.73. We found slightly larger communities with the best-fit conductance, while the baselines found smaller communities with lower conductance. This may explain why our detection accuracy on Orkut is slightly lower.

For the three Biology datasets, every variant of LOSP outperforms the baselines, except for LRw on DM. Also, the conductance of the communities detected by LOSP (around 0.75) is very close to that of the ground truth (around 0.88, as shown in Table 2). As for the community size, we detected larger communities as compared to the ground truth, but the baselines detect even larger communities.

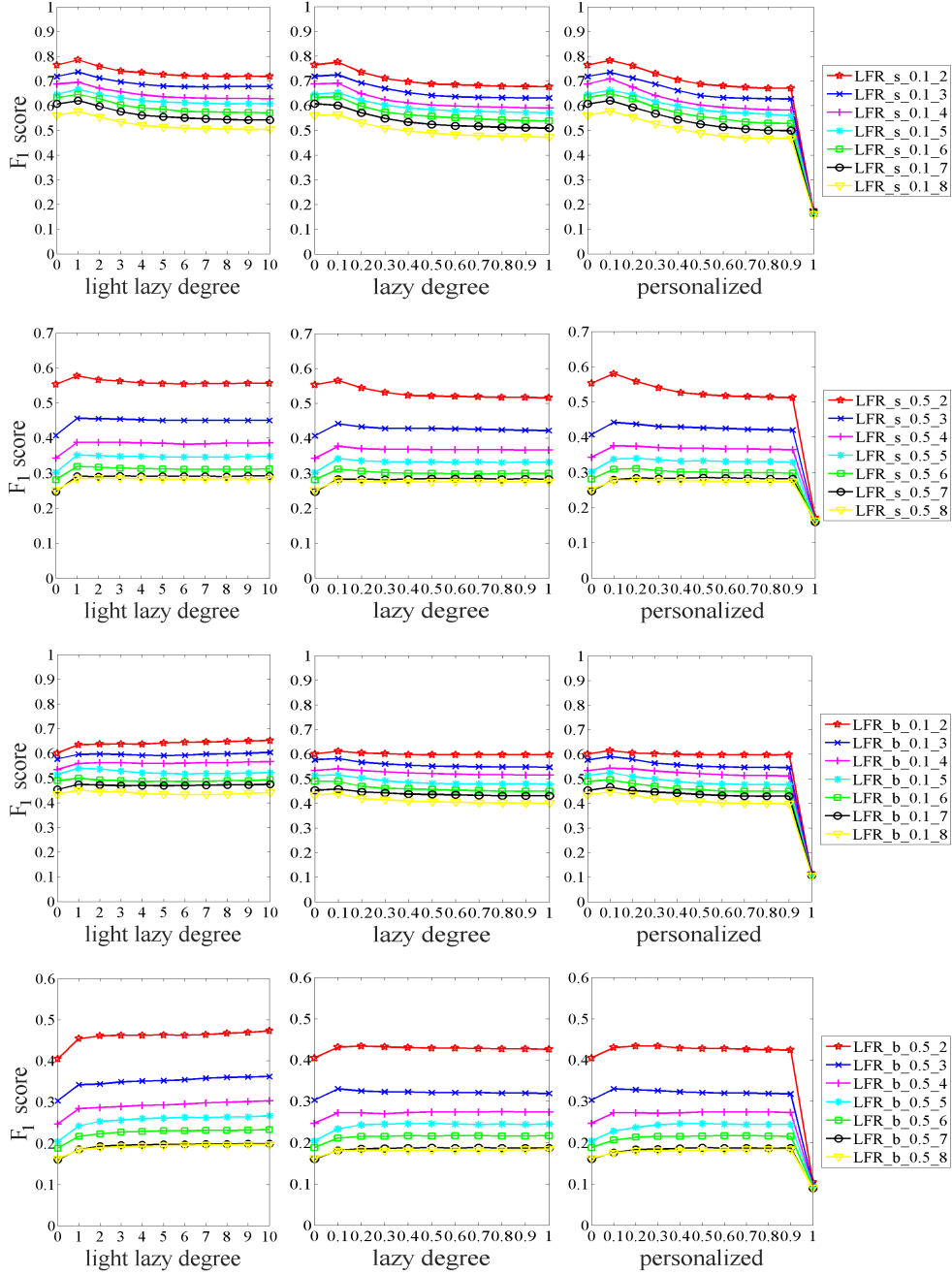


Fig. 2. Evaluation of different diffusion parameters on LFR datasets (Defined on N_{rw}^T Krylov subspace, community size truncated by truth size). The three diffusions are robust for different α parameters, except for $\alpha = 1$ on personalized pagerank, in which case all probability returns to the original seed set.

For the running time, as shown in Table 8, LOSP is fast in 4 seconds on SNAP and in 15 seconds on Biology dataset. The two baselines, HK and PR, are faster in less than 1 seconds. This may due to that LOSP is implemented in Matlab while the baselines are implemented in C++. Also, LOSP needs to find the local minimum of the conductance to determine the community boundary, leading more time especially on larger communities.

5.4.2 Comparison on LFR Datasets

For each of synthetic LFR datasets, Table 7 shows the average detection accuracy and conductance of the detected

communities, Table 9 shows the average community size and running time.

For the four sets with a total of 28 LFR datasets, LOSP clearly outperform the state of the art baselines, HK and PR. Specifically:

- **LFR_s_0.1.** The size of the ground truth is in [10, 50], and the average conductance of the ground truth is 0.522. The average detection size of LOSP over the seven LFR_s_0.1 datasets is suitable in [16, 41], while the baselines detect much larger communities in 2300. Due to the difference on the detected size, LOSP is high around 0.70 while the baselines is low around 0.29 in conductance.

TABLE 6

Comparison on detection accuracy and conductance with heat kernel (HK) and pagerank (PR) on real-world networks (on N_{rw}^T).

		F_1 score						Conductance					
		LRw	LLi	LLa	LPr	HK	PR	LRw	LLi	LLa	LPr	HK	PR
SNAP	Amazon	0.797	0.800	0.762	0.769	0.751	0.531	0.322	0.300	0.352	0.354	0.042	0.030
	DBLP	0.763	0.779	0.752	0.748	0.413	0.388	0.444	0.396	0.475	0.477	0.110	0.114
	LiveJ	0.782	0.797	0.753	0.767	0.573	0.525	0.335	0.305	0.383	0.368	0.083	0.086
	YouTube	0.342	0.445	0.466	0.460	0.091	0.143	0.812	0.736	0.795	0.809	0.175	0.302
	Orkut	0.282	0.279	0.264	0.277	0.357	0.303	0.796	0.791	0.808	0.798	0.513	0.546
Average		0.593	0.620	0.599	0.604	0.437	0.378	0.542	0.506	0.563	0.561	0.185	0.216
Biology	DM	0.198	0.221	0.253	0.235	0.219	0.035	0.761	0.772	0.757	0.793	0.571	0.181
	HS	0.157	0.206	0.186	0.171	0.025	0.020	0.710	0.758	0.757	0.755	0.229	0.080
	SC	0.096	0.120	0.180	0.108	0.036	0.034	0.677	0.696	0.727	0.688	0.322	0.343
	Average	0.150	0.182	0.206	0.171	0.093	0.030	0.716	0.742	0.747	0.745	0.374	0.201

TABLE 7

Comparison on detection accuracy and conductance with heat kernel (HK) and pagerank (PR) on LFR networks (on N_{rw}^T).

		F_1 score						Conductance					
		LRw	LLi	LLa	LPr	HK	PR	LRw	LLi	LLa	LPr	HK	PR
LFR	s_0.1_2	0.664	0.673	0.510	0.673	0.051	0.025	0.595	0.557	0.693	0.567	0.276	0.269
	s_0.1_3	0.613	0.621	0.485	0.622	0.028	0.025	0.649	0.598	0.717	0.617	0.289	0.281
	s_0.1_4	0.567	0.583	0.463	0.566	0.027	0.024	0.681	0.619	0.742	0.657	0.294	0.286
	s_0.1_5	0.535	0.555	0.433	0.534	0.044	0.024	0.705	0.636	0.755	0.682	0.300	0.290
	s_0.1_6	0.524	0.548	0.414	0.541	0.026	0.024	0.693	0.627	0.755	0.657	0.295	0.294
	s_0.1_7	0.513	0.536	0.407	0.518	0.041	0.026	0.717	0.644	0.763	0.689	0.300	0.297
	s_0.1_8	0.459	0.503	0.391	0.476	0.029	0.024	0.737	0.666	0.768	0.721	0.305	0.302
	Average	0.554	0.574	0.443	0.561	0.035	0.025	0.682	0.621	0.742	0.656	0.294	0.288
	s_0.5_2	0.458	0.496	0.418	0.483	0.019	0.020	0.804	0.741	0.804	0.786	0.333	0.324
	s_0.5_3	0.306	0.388	0.334	0.356	0.020	0.022	0.818	0.789	0.814	0.849	0.348	0.346
	s_0.5_4	0.229	0.336	0.274	0.296	0.019	0.020	0.794	0.801	0.792	0.854	0.359	0.357
	s_0.5_5	0.196	0.313	0.240	0.270	0.018	0.019	0.786	0.814	0.790	0.847	0.362	0.363
	s_0.5_6	0.174	0.284	0.213	0.235	0.017	0.018	0.782	0.813	0.783	0.837	0.355	0.368
	s_0.5_7	0.131	0.260	0.182	0.199	0.017	0.018	0.753	0.817	0.766	0.825	0.358	0.371
	s_0.5_8	0.132	0.260	0.191	0.201	0.016	0.017	0.741	0.812	0.772	0.821	0.368	0.374
	Average	0.232	0.334	0.265	0.291	0.018	0.019	0.783	0.798	0.789	0.831	0.355	0.358
	b_0.1_2	0.411	0.461	0.319	0.437	0.094	0.040	0.754	0.666	0.778	0.704	0.303	0.286
	b_0.1_3	0.412	0.417	0.329	0.406	0.064	0.043	0.735	0.688	0.759	0.717	0.307	0.295
	b_0.1_4	0.359	0.392	0.306	0.370	0.092	0.039	0.772	0.702	0.765	0.748	0.308	0.295
	b_0.1_5	0.338	0.361	0.288	0.336	0.073	0.042	0.794	0.716	0.787	0.771	0.301	0.300
	b_0.1_6	0.335	0.374	0.289	0.338	0.060	0.038	0.752	0.698	0.779	0.748	0.296	0.301
	b_0.1_7	0.334	0.353	0.280	0.331	0.047	0.039	0.768	0.710	0.774	0.735	0.296	0.301
	b_0.1_8	0.318	0.349	0.262	0.336	0.051	0.038	0.780	0.714	0.781	0.752	0.312	0.304
	Average	0.358	0.387	0.296	0.365	0.069	0.040	0.765	0.699	0.775	0.739	0.303	0.297
	b_0.5_2	0.246	0.309	0.277	0.276	0.040	0.042	0.805	0.792	0.811	0.833	0.343	0.336
	b_0.5_3	0.190	0.236	0.199	0.214	0.039	0.041	0.793	0.808	0.794	0.857	0.340	0.355
	b_0.5_4	0.135	0.198	0.163	0.175	0.035	0.037	0.749	0.813	0.779	0.830	0.353	0.362
	b_0.5_5	0.106	0.177	0.149	0.148	0.033	0.036	0.739	0.815	0.794	0.827	0.373	0.365
	b_0.5_6	0.101	0.170	0.138	0.136	0.031	0.033	0.735	0.817	0.783	0.821	0.359	0.368
	b_0.5_7	0.076	0.150	0.123	0.117	0.031	0.033	0.687	0.810	0.767	0.785	0.363	0.369
	b_0.5_8	0.082	0.149	0.125	0.120	0.030	0.032	0.711	0.804	0.768	0.803	0.363	0.370
	Average	0.134	0.198	0.168	0.169	0.034	0.036	0.746	0.808	0.785	0.822	0.356	0.361

TABLE 8

Comparison on community size and running time with heat kernel (HK) and pagerank (PR) on real-world networks (on N_{rw}^T).

		Size						Time (s)					
		LRw	LLi	LLa	LPr	HK	PR	LRw	LLi	LLa	LPr	HK	PR
SNAP	Amazon	7	8	7	7	48	4485	0.010	0.011	0.009	0.008	0.008	0.015
	DBLP	10	10	8	8	87	9077	0.086	0.099	0.087	0.083	0.025	0.075
	LiveJ	34	35	30	29	119	512	0.634	0.756	0.718	0.715	0.029	0.264
	YouTube	712	588	575	632	122	13840	8.433	9.268	8.905	9.299	0.038	0.955
	Orkut	1269	1733	1583	1833	341	1648	10.625	12.235	12.189	12.536	0.027	1.392
Average		406	475	441	502	143	5912	3.958	4.474	4.382	4.528	0.025	0.540
Biology	DM	1120	992	721	748	606	15120	27.062	33.535	33.156	30.835	0.015	1.394
	HS	965	465	626	609	4360	10144	3.444	3.823	3.688	3.948	0.071	1.048
	SC	1642	1623	1045	1434	2604	2673	9.526	11.119	10.528	10.754	0.034	0.979
	Average	1242	1027	797	930	2523	9312	13.344	16.159	15.791	15.179	0.040	1.140

TABLE 9
Comparison on community size and running time with heat kernel(HK) and pagerank(PR) on LFR networks (on N_{rw}^T).

	Size						Time (s)						
	LRw	LLi	LLa	LPr	HK	PR	LRw	LLi	LLa	LPr	HK	PR	
LFR	s_0.1_2	12	13	9	12	2279	2327	0.777	0.918	0.864	0.882	0.025	0.692
	s_0.1_3	11	12	9	11	2356	2317	0.821	0.969	0.959	0.958	0.025	0.693
	s_0.1_4	13	11	8	12	2354	2318	0.870	1.022	1.002	1.005	0.025	0.690
	s_0.1_5	17	11	36	9	2363	2328	0.978	1.123	1.126	1.110	0.026	0.675
	s_0.1_6	33	34	54	18	2387	2302	1.107	1.269	1.288	1.284	0.025	0.682
	s_0.1_7	31	22	77	21	2349	2272	1.222	1.342	1.385	1.353	0.025	0.677
	s_0.1_8	80	39	95	28	2371	2278	1.261	1.371	1.413	1.421	0.025	0.678
	Average	28	20	41	16	2351	2306	1.005	1.145	1.148	1.145	0.025	0.684
	s_0.5_2	57	49	32	20	2420	2313	1.124	1.232	1.219	1.274	0.028	0.680
s_0.5_3	283	76	156	102	2456	2281	1.447	1.626	1.602	1.633	0.026	0.686	
s_0.5_4	529	121	401	204	2459	2258	1.511	1.708	1.694	1.690	0.028	0.683	
s_0.5_5	687	129	516	303	2463	2246	1.678	1.949	1.877	1.903	0.028	0.687	
s_0.5_6	751	210	611	372	2384	2242	1.698	1.899	1.880	1.942	0.027	0.690	
s_0.5_7	904	213	697	490	2374	2231	1.764	1.914	1.822	1.854	0.027	0.694	
s_0.5_8	986	220	679	517	2304	2230	1.923	2.037	1.975	2.043	0.025	0.696	
Average	600	145	442	287	2409	2257	1.592	1.766	1.724	1.763	0.027	0.688	
b	b_0.1_2	12	16	11	13	2258	2344	0.995	1.089	1.050	0.944	0.026	0.737
	b_0.1_3	25	15	31	12	2368	2340	1.146	1.253	1.193	1.192	0.025	0.720
	b_0.1_4	76	22	109	24	2267	2343	1.433	1.424	1.415	1.248	0.025	0.717
	b_0.1_5	52	25	69	17	2354	2334	1.350	1.595	1.488	1.571	0.025	0.713
	b_0.1_6	100	50	89	69	2374	2323	1.429	1.640	1.614	1.651	0.025	0.718
	b_0.1_7	117	29	156	114	2417	2326	1.341	1.608	1.581	1.599	0.025	0.714
	b_0.1_8	82	40	160	72	2374	2330	1.362	1.597	1.593	1.619	0.025	0.721
	Average	66	28	89	46	2344	2334	1.294	1.458	1.419	1.403	0.025	0.720
	b_0.5_2	321	33	147	105	2465	2299	1.412	1.579	1.560	1.679	0.025	0.718
b_0.5_3	567	106	364	178	2430	2280	1.658	1.858	1.878	1.875	0.025	0.706	
b_0.5_4	825	237	577	413	2440	2252	1.806	2.026	2.015	1.999	0.025	0.701	
b_0.5_5	804	184	472	424	2473	2242	1.561	1.818	1.781	1.781	0.025	0.689	
b_0.5_6	964	196	590	511	2425	2240	1.751	2.079	2.008	2.021	0.025	0.705	
b_0.5_7	1224	247	705	654	2415	2224	1.828	2.123	2.079	2.068	0.025	0.704	
b_0.5_8	1050	268	677	569	2406	2221	1.805	2.116	2.093	2.088	0.025	0.703	
Average	822	182	505	408	2436	2251	1.689	1.943	1.916	1.930	0.025	0.704	

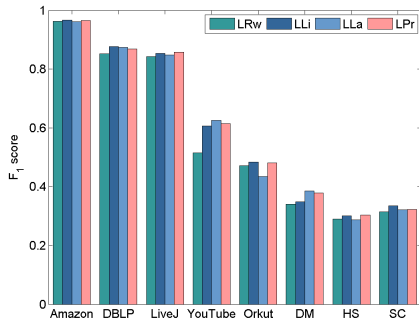


Fig. 3. Accuracy evaluation of LOASP on real-world networks (Defined on N_{rw}^T Krylov subspace, community size truncated by truth size). LOASPs based on the four diffusions show similar accuracy over all datasets.

- **LFR_s_0.5**. The size of the ground truth is in [10, 50], and the average conductance of the ground truth is 0.746. The average detection size of LOASP is considerably larger in [145, 600], and the conductance is very close to that of the ground truth. HK and PR still find much larger communities, leading to apparently smaller conductance.
- **LFR_b_0.1**. The size of the ground truth is in [20, 100], and the average conductance of the ground truth is 0.497. The average detection size of LOASP is suitable in [28, 89], while the baselines detect much larger communities in 2300. Due to the difference on the detected

size, LOASP is high around 0.74 while the baselines is low around 0.30 in conductance.

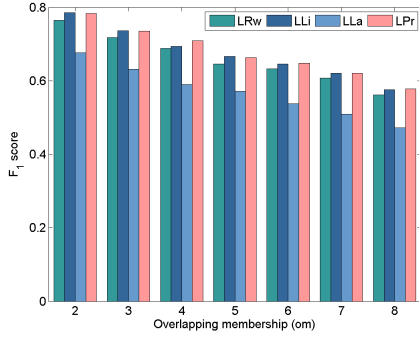
- **LFR_b_0.5**. The size of the ground truth is in [20, 100], and the average conductance of the ground truth is 0.733. The average detection size of LOASP is considerably larger in [182, 822], and the conductance is very close to that of the ground truth. HK and PR still find much larger communities, leading to apparently smaller conductance.

It is reasonable that the detection accuracy decays on graphs where there exist more overlappings indicated by higher om and on . LOASP substantially outperforms HK and PR. HK and PR tend to find much-larger-size communities with lower-conductance and their detection accuracy is very low, which is less than 0.07 on average on each of the four group datasets.

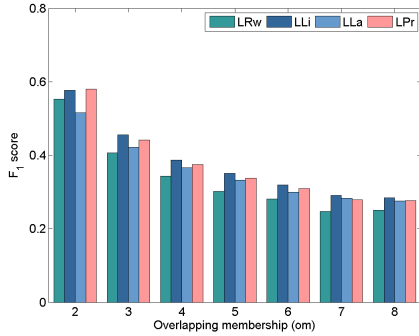
For the running time, as shown in Table 9, LOASP is fast in 1 to 2 seconds while the two baselines, HK and PR are faster in less than 1 seconds. This may due to the difference on programming language implementation and the method for determining the community boundary.

6 CONCLUSION

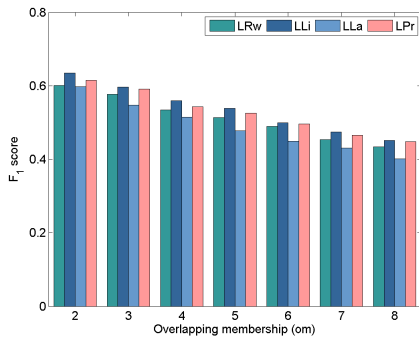
This paper systematically explores a family of local spectral methods (LOSP) for finding members of a local community from a few randomly selected seed members. Based on a Krylov subspace approximation, we define “approximate



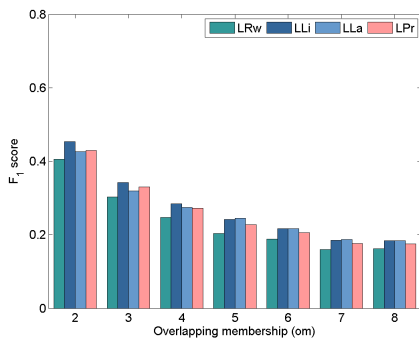
(a) LFR_s_0.1



(b) LFR_s_0.5



(c) LFR_b_0.1



(d) LFR_b_0.5

Fig. 4. Accuracy evaluation of LOSP on LFR networks (Defined on $N_{\tau_w}^T$ Krylov subspace, community size truncated by truth size). The accuracy decays with larger om values. The four diffusions show similar accuracy over all datasets. LLI and LPr, LOSP with light lazy or pagerank diffusion, demonstrate slightly higher accuracy.

eigenvectors” for a subgraph including a neighborhood around the seeds, and describe how to extract a community from these approximate eigenvectors. By using different

seed sets that generate different subspaces, our method is capable of finding overlapping communities.

Variants of LOSP are introduced and evaluated. Four types of random walks with different diffusion speeds are studied, regular random walk and inverse random walk are compared, and analysis on the conductance bounding of the target community is provided. For this semi-supervised learning task, LOSP outperforms prior state-of-the-art local community detection methods in social and biological networks as well as synthetic LFR datasets.

The extension of the LOSP approach to directed and weighted networks will be the subject of future work.

ACKNOWLEDGMENTS

This paper is a significant extension of the ICDM conference paper [15]. This work was supported by National Natural Science Foundation of China (61772219, 61472147, 61602196), US Army Research Office (W911NF-14-1-0477), and MSRA Collaborative Research (97354136).

REFERENCES

- [1] G. Palla, I. Derényi, I. Farkas, and T. Vicsek, “Uncovering the overlapping community structure of complex networks in nature and society,” *Nature*, vol. 435, no. 7043, pp. 814–818, 2005.
- [2] Y.-Y. Ahn, J. P. Bagrow, and S. Lehmann, “Link communities reveal multiscale complexity in networks,” *Nature*, vol. 466, no. 7307, pp. 761–764, 2010.
- [3] J. Yang and J. Leskovec, “Defining and evaluating network communities based on ground-truth,” in *ICDM*, December 2012, pp. 745–754.
- [4] I. M. Kloumann and J. M. Kleinberg, “Community membership identification from small seed sets,” in *KDD*. ACM, August 2014, pp. 1366–1375.
- [5] Y. Wu, R. Jin, J. Li, and X. Zhang, “Robust local community detection: on free rider effect and its elimination,” in *VLDB*, August 2015, pp. 798–809.
- [6] T. van Laarhoven and E. Marchiori, “Local network community detection with continuous optimization of conductance and weighted kernel k-means,” *The Journal of Machine Learning Research*, vol. 17, pp. 5148–5175, 2016.
- [7] I. Weber, V. R. K. Garimella, and A. Batayneh, “Secular vs. Islamist polarization in Egypt on Twitter,” in *ASONAM*, 2013, pp. 290–297.
- [8] J. Leskovec, K. J. Lang, A. Dasgupta, and M. W. Mahoney, “Statistical properties of community structure in large social and information networks,” in *WWW*, 2008, pp. 695–704.
- [9] Y. Han and J. Tang, “Probabilistic community and role model for social networks,” in *Proceedings of the 21th ACM SIGKDD International Conference on Knowledge Discovery and Data Mining*. ACM, 2015, pp. 407–416.
- [10] A. Lancichinetti, F. Radicchi, J. J. Ramasco, and S. Fortunato, “Finding statistically significant communities in networks,” *PLoS ONE*, vol. 6, no. 4, p. e18961, 2011.
- [11] J. J. Whang, D. F. Gleich, and I. S. Dhillon, “Overlapping community detection using seed set expansion,” in *CIKM*, October 2013, pp. 2099–2108.
- [12] K. Kloster and D. F. Gleich, “Heat kernel based community detection,” in *KDD*. ACM, August 2014, pp. 1386–1395.
- [13] R. Andersen, F. Chung, and K. Lang, “Local graph partitioning using PageRank vectors,” in *FOCS*, 2006, pp. 475–486.
- [14] F. Chung and O. Simpson, “Solving linear systems with boundary conditions using heat kernel PageRank,” in *Algorithms and Models for the Web Graph (WAW)*, 2013, pp. 203–219.
- [15] K. He, Y. Sun, D. Bindel, J. E. Hopcroft, and Y. Li, “Detecting overlapping communities from local spectral subspaces,” in *ICDM*, 2015, pp. 769–774.
- [16] Y. Li, K. He, D. Bindel, and J. E. Hopcroft, “Uncovering the small community structure in large networks,” in *WWW*, 2015, pp. 658–668.

- [17] M. E. J. Newman, "Modularity and community structure in networks," *Proceedings of the National Academy of Sciences*, vol. 103, no. 23, pp. 8577–8582, 2006.
- [18] J. Shi and J. Malik, "Normalized cuts and image segmentation," *IEEE Trans. Pattern Analysis and Machine Intelligence*, vol. 22, no. 8, pp. 888–905, 2000.
- [19] S. Fortunato and C. Castellano, "Community structure in graphs," *Computational Complexity*, pp. 490–512, 2012.
- [20] S. Papadopoulos, Y. Kompatsiaris, A. Vakali, and P. Spyridonos, "Community detection in social media," *Data Mining and Knowledge Discovery*, vol. 24, no. 3, pp. 515–554, 2012.
- [21] J. Xie, S. Kelley, and B. K. Szymanski, "Overlapping community detection in networks: The state-of-the-art and comparative study," *ACM Computing Surveys (CSUR)*, vol. 45, no. 4, p. 43, 2013.
- [22] M. Coscia, G. Rossetti, F. Giannotti, and D. Pedreschi, "Demon: a local-first discovery method for overlapping communities," in *KDD*. ACM, 2012, pp. 615–623.
- [23] M. W. Mahoney, L. Orecchia, and N. K. Vishnoi, "A local spectral method for graphs: with applications to improving graph partitions and exploring data graphs locally," *The Journal of Machine Learning Research*, vol. 13, no. 1, pp. 2339–2365, 2012.
- [24] X. Ma and D. Dong, "Evolutionary nonnegative matrix factorization algorithms for community detection in dynamic networks," *IEEE Trans. Knowl. Data Eng.*, vol. 29, no. 5, pp. 1045–1058, 2017.
- [25] L. Wu, X. Wu, A. Lu, and Y. Li, "On spectral analysis of signed and dispartite graphs: Application to community structure," *IEEE Trans. Knowl. Data Eng.*, vol. 29, no. 7, pp. 1480–1493, 2017.
- [26] A. Mahmood and M. Small, "Subspace based network community detection using sparse linear coding," *IEEE Trans. Knowl. Data Eng.*, vol. 28, no. 3, pp. 801–812, 2016.
- [27] A. Prat-Pérez, D. Dominguez-Sal, J. M. Brunat, and J. Larriba-Pey, "Put three and three together: Triangle-driven community detection," *TKDD*, vol. 10, no. 3, pp. 22:1–22:42, 2016.
- [28] J. J. Whang, D. F. Gleich, and I. S. Dhillon, "Overlapping community detection using neighborhood-inflated seed expansion," *IEEE Trans. Knowl. Data Eng.*, vol. 28, no. 5, pp. 1272–1284, 2016.
- [29] S. Soundarajan and J. E. Hopcroft, "Use of local group information to identify communities in networks," *TKDD*, vol. 9, no. 3, pp. 21:1–21:27, 2015.
- [30] M. E. J. Newman, "Spectral methods for network community detection and graph partitioning," *Physical Review E*, vol. 88, no. 4, p. 042822, 2013.
- [31] R. Andersen and K. J. Lang, "Communities from seed sets," in *WWW*. ACM, 2006, pp. 223–232.
- [32] B. Abrahao, S. Soundarajan, J. E. Hopcroft, and R. Kleinberg, "A separability framework for analyzing community structure," *ACM Transactions on Knowledge Discovery from Data (TKDD)*, vol. 8, no. 1, p. 5, 2014.
- [33] D. A. Spielman and S. Teng, "Nearly-linear time algorithms for graph partitioning, graph sparsification, and solving linear systems," in *STOC*, 2004, pp. 81–90.
- [34] F. Chung, "The heat kernel as the PageRank of a graph," *PNAS*, vol. 104, no. 50, pp. 19735–19740, 2007.
- [35] —, "A local graph partitioning algorithm using heat kernel PageRank," *Internet Mathematics*, vol. 6, no. 3, pp. 315–330, 2009.
- [36] U. von Luxburg, "A tutorial on spectral clustering," *Statistics and Computing*, vol. 17, no. 4, pp. 395–416, 2007.
- [37] R. Kannan, S. Vempala, and A. Vetta, "On clusterings - good, bad and spectral," in *FOCS*, 2000, pp. 367–377.
- [38] A. Lancichinetti, S. Fortunato, and F. Radicchi, "Benchmark graphs for testing community detection algorithms," *Physical Review E*, vol. 78, no. 4, p. 046110, 2008.
- [39] A. Lancichinetti and S. Fortunato, "Benchmarks for testing community detection algorithms on directed and weighted graphs with overlapping communities," *Physical Review E*, vol. 80, no. 1, p. 016118, 2009.
- [40] F. Chung, *Spectral graph theory*. American Mathematical Soc., 1997.
- [41] G. H. Golub and C. F. V. Loan, *Matrix computations (3. ed.)*. Johns Hopkins University Press, 1996.



Kun He is currently a professor in the Department of Computer Science, Huazhong University of Science and Technology (HUST), Wuhan, P.R. China; and a Mary Shepard B. Upton Visiting Professor for the 2016-2017 Academic year in Engineering, Cornell University, NY, USA. She received her Ph.D. degree in the Department of Automatic Control from HUST in 2006, Wuhan, P.R. China. Her major research interests include algorithm design and analysis, machine learning and data mining. More specifically, she has worked on the community detection algorithms in complex networks, algorithms for NP hard problems, and understanding the deep representation of neural networks.



Pan Shi is currently a Ph.D. student in the Department of Computer Science, Huazhong University of Science and Technology (HUST), Wuhan, P.R. China. His research interests include data mining in complex networks.



David Bindel is currently an associate professor in Computer Science, Cornell University, NY, USA. He received the Ph.D. degree in computer science from the University of California at Berkeley in 2006, and his dissertation was awarded the Householder Prize for most outstanding dissertation in numerical linear algebra over the past three years in 2008. His major research interests include making grids smarter, spectral network analysis, nonlinear eigenvalue bounds and parallel surrogate optimization.



John E. Hopcroft is the IBM Professor of Engineering and Applied Mathematics in Computer Science at Cornell University. He has coauthored four books on formal languages and algorithms with Jeffrey D. Ullman and Alfred V. Aho. He was honored with the A. M. Turing Award in 1986. He is a member of the National Academy of Sciences (NAS), the National Academy of Engineering (NAE) and a fellow of the American Academy of Arts and Sciences (AAAS), the American Association for the Advancement of

Science, the Institute of Electrical and Electronics Engineers (IEEE), and the Association of Computing Machinery (ACM). Hopcroft's research centers on theoretical aspects of computing, especially analysis of algorithms, automata theory, and graph algorithms. His most recent work is on the study of information capture and access.